84-2-117

EUROPEAN ORGANIZATION FOR NUCLEAR RESEARCH

CERN-EP/83-198
22 December 1983

ANGULAR DISTRIBUTIONS AND STRUCTURE FUNCTIONS FROM TWO-JET EVENTS AT THE CERN SPS $p\bar{p}$ COLLIDER

UA1 Collaboration, CERN, Geneva, Switzerland

Aachen[1]–Annecy (LAPP)[2]–Birmingham[3]–CERN[4]–Helsinki[5]– Queen Mary College, London[6]–
Paris (Coll. de France)[7]–Riverside[8]–Rome[9]–Rutherford Appleton Lab.[10]–
Saclay (CEN)[11]–Vienna[12] Collaboration

G. Arnison[10], A. Astbury[10], B. Aubert[2], C. Bacci[9], G. Bauer**, A. Bézaguet[4], R.K. Bock[4], T.J.V. Bowcock[6], M. Calvetti[4], T. Carroll[4], P. Catz[2], P. Cennini[4], S. Centro[4], F. Ceradini[4,9], S. Cittolin[4], D. Cline**, C. Cochet[11], J. Colas[2], M. Corden[3], D. Dallman[4,12], M. DeBeer[11], M. Della Negra[2,4], M. Demoulin[4], D. Denegri[11], A. Di Ciaccio[9], D. DiBitonto[4], L. Dobrzynski[7], J.D. Dowell[3], K. Eggert[1], E. Eisenhandler[6], N. Ellis[4], P. Erhard[1], H. Faissner[1], G. Fontaine[7], R. Frey[8], R. Frühwirth[12], J. Garvey[3], S. Geer[7], C. Ghesquière[7], P. Ghez[2], K.L. Giboni[1], W.R. Gibson[6], Y. Giraud-Héraud[7], A. Givernaud[11], A. Gonidec[2], G. Grayer[10], P. Gutierrez[8], T. Hansl-Kozanecka[1], W.J. Haynes[10], L.O. Hertzberger*, C. Hodges[8], D. Hoffmann[1], H. Hoffmann[4], D.J. Holthuizen*, R.J. Homer[3], A. Honma[6], W. Jank[4], G. Jorat[4], P.I.P. Kalmus[6], V. Karimäki[5], R. Keeler[6], I. Kenyon[3], A. Kernan[8], R. Kinnunen[5], H. Kowalski[4], W. Kozanecki[8], D. Kryn[4,7], P. Kyberd[6], F. Lacava[4], J.-P. Laugier[11], J.-P. Lees[2], H. Lehmann[1], K. Leuchs[1], A. Lévêque[11,4], D. Linglin[2], E. Locci[11], M. Loret[11], J.-J. Malosse[11], T. Markiewicz[4], G. Maurin[4], T. McMahon[3], J.-P. Mendiburu[7], M.-N. Minard[2], M. Moricca[9], H. Muirhead***, F. Muller[4], A.K. Nandi[10], L. Naumann[4], A. Norton[4], A. Orkin-Lecourtois[7], L. Paoluzi[9], G. Piano Mortari[9], E. Pietarinen[5], M. Pimiä[5], A. Placci[4], E. Radermacher[1], J. Ransdell[8], H. Reithler[1], J.-P. Revol[4], J. Rich[11], M. Rijssenbeek[4], C. Roberts[10], J. Rohlf[4], P. Rossi[4], C. Rubbia[4], B. Sadoulet[4], G. Sajot[7], G. Salvi[6], G. Salvini[9], J. Sass[11], J. Saudraix[11], A. Savoy-Navarro[11], D. Schinzel[4], W. Scott[10], T.P. Shah[10], D. Smith[8], M. Spiro[11], J. Strauss[12], K. Sumorok[4], F. Szoncso[12], C. Tao*, G. Thompson[6], J. Timmer[4], E. Tscheslog[1], J. Tuominiemi[5], J.-P. Vialle[4], J. Vrana[7], V. Vuillemin[4], H.D. Wahl[12], P. Watkins[3], J. Wilson[3], Y.G. Xie[4], M. Yvert[2], E. Zurfluh[4]

(Submitted to Physics Letters)

---

*) NIKHEF, Amsterdam, The Netherlands.
**) University of Wisconsin, Madison, Wisconsin, USA.
***) Visitor from the University of Liverpool, England.

ABSTRACT

The two-jet cross-section measured in the UA1 apparatus at the CERN $p\bar{p}$ Collider has been analysed in terms of the centre-of-mass scattering angle θ and the scaled longitudinal parton momenta x_1 and x_2. The angular distribution $d\sigma/d\cos\theta$ rises rapidly as $\cos\theta \to 1$, independent of x_1 and x_2, as expected in vector gluon theories (QCD). The differential cross-section in x_1 and x_2 is consistent with factorization and provides a measurement of the proton structure function $F(x) = G(x) + (4/9)\,[Q(x) + \bar{Q}(x)]$ at values of the 4-momentum transfer squared, $-\hat{t} \approx 2000\ \mathrm{GeV}^2$. Over the range $x = 0.10$–0.80 the structure function shows an exponential x dependence and may be parametrized by the form $F(x) = 6.2\,e^{-9.5x}$.

The observation [1,2] of well-defined two-jet events in proton–antiproton collisions at high energy opens up the possibility of proton structure function measurements at values of four-momentum transfer squared (Q^2) in excess of 2000 GeV^2, far higher than previously accessible using lepton beams. In the parton model two-jet events result when an incoming parton from the antiproton and an incoming parton from the proton interact with each other to produce two outgoing high transverse momentum partons which are observed as jets.

If $d\sigma/d\cos\theta$ is the differential cross-section for a particular parton–parton subprocess as a function of the c.m.s. scattering angle θ, the corresponding contribution to the two jet cross-section may be written:

$$d^3\sigma/dx_1dx_2d\cos\theta = [F(x_1)/x_1]\,[F(x_2)/x_2]\,d\sigma/d\cos\theta\,, \tag{1}$$

where $F(x_1)/x_1$ $[F(x_2)/x_2]$ is a structure function representing the number density of the appropriate partons in the antiproton [proton] as a function of the scaled longitudinal momentum $x_1[x_2]$ of the partons.

The differential cross-sections for the possible subprocess have been calculated to leading order in QCD [3]. The elastic scattering subprocesses [gluon–gluon, gluon–quark(antiquark) and quark(antiquark)–quark(antiquark)] have a similar angular dependence and become large as $\cos\theta \to 1$ [like $(1-\cos\theta)^{-2}$] as a consequence of vector gluon exchange. In the approximation that the elastic subprocesses dominate and have a common angular dependence, the total two-jet cross-section may be written in the form of eq. (1) [4]. In particular, if $d\sigma/d\cos\theta$ is taken to be the differential cross-section for gluon–gluon elastic scattering:

$$d\sigma/d\cos\theta = (9/8)\,[\pi a_s^2/2x_1x_2s]\,(3+\cos^2\theta)^3\,(1-\cos^2\theta)^{-2}\,, \tag{2}$$

where a_s is the QCD coupling constant and s is the total c.m.s. energy squared, then the structure function F(x) becomes:

$$F(x) = G(x) + (4/9)\,[Q(x) + \bar{Q}(x)]\,, \tag{3}$$

where G(x), Q(x), and $\bar{Q}(x)$ are respectively the gluon, quark, and antiquark structure functions of the proton. In eq. (3) the factor 4/9 reflects the relative strengths of the quark–gluon and gluon–gluon couplings predicted by QCD.

In this paper the experimental angular distribution of jet pairs produced in $p\bar{p}$ collisions is analysed as a test of vector gluon exchange and results are presented on the structure function F(x) defined by eqs. (1)–(3). The initial data sample comprises all jet triggers in the UA1 apparatus corresponding to an integrated luminosity of $\approx$ 15 nb^{-1} taken during the 1982 runs at the CERN SPS $p\bar{p}$ Collider ($\sqrt{s}$ = 540 GeV).

For the 1982 runs the UA1 jet trigger [5] required $\geq$ 1 localized transverse energy (E_T) deposition with $E_T > 15$ GeV in the central-barrel calorimetry (pseudorapidity $|\eta| < 1.5$). A localized transverse energy deposition was defined by a window comprising any two adjacent hadronic calorimeter elements summed with the corresponding electromagnetic calorimeter elements subtending an aperture $\Delta\eta \approx 0.75, \Delta\phi \approx \pi$ radians, where ϕ is the azimuthal angle around the beam direction. Two data sets were prepared from the raw data tapes: i) a filtered data set corresponding to an integrated luminosity of 14.2 nb^{-1}, for which the trigger threshold requirement was redefined to be $E_T > 25$ GeV using an off-line filter programme; ii) an unfiltered data set

corresponding to an integrated luminosity of 0.7 nb^{-1}, for which the trigger threshold remains as defined by the hardware trigger. The results presented below are based on the analysis of the filtered and unfiltered data sets combined.

A set of Monte Carlo events [6] generated using ISAJET [7] has been analysed in parallel with the real data. ISAJET generates two jet events and simulates the fragmentation of each jet into hadrons including the effects of QCD bremsstrahlung. The Monte Carlo program simulates in detail the subsequent behaviour of the hadrons in the UA1 apparatus. The Monte Carlo events are used to calculate various corrections which are discussed below, and to estimate the jet energy resolution and the uncertainty in the determination of the jet direction.

After full calorimeter reconstruction jets are defined using the UA1 jet algorithm [5]. The energy and momentum of each jet is computed by taking respectively the scalar and vector sum over the associated calorimeter cells. A correction is applied to the measured energy ($\approx +10\%$) and momentum ($\approx +6\%$) of each jet, as a function of the pseudorapidity and azimuth of the jet,on the basis of the Monte Carlo analysis, to account for the effect of uninstrumented material and containment losses.

After jet finding, events are selected with ≥ 2 jets, within the acceptance of the central calorimetry $|\eta| < 3$. While the majority of these events have a topology consistent with two balanced high E_T jets, some 10–15% of the events have additional jets with $E_T > 15$ GeV [5]. A preceding analysis [5] has shown that multijet events are largely accounted for in terms of initial- and final-state bremsstrahlung processes [8]. For this analysis, in order to compare with theoretical expectations for the two-jet cross-section, additional jets, apart from the two highest E_T jets, are ignored. The r.m.s. transverse momentum of the two-jet system (taking account of resolution) is then $\approx$ 10 GeV. A further correction is then applied, on the basis of the Monte Carlo analysis, to the energy ($\approx +12\%$) and momentum ($\approx +7\%$) of the two highest E_T jets in order to account for final state radiation falling outside the jet, as defined oy the jet algorithm. In the forward direction ($|\eta| \gtrsim 1.5$) it is found that the jet axis as defined by the jet algorithm is systematically shifted towards the beams due to the misassignment of beam fragments as part of the jet. The magnitude of this shift is ≈ 0.07 radians and a correction is made to the measured jet angles to account for this effect. After all corrections, averaged over the full acceptance, the jet energy resolution $\delta E/E \approx \pm 26\%$ and the uncertainty in the jet direction (in pseudorapidity) $\delta\eta \approx \pm 0.05$.

For each event the x_1 and x_2 of the interacting partons are computed as follows:

$$x_1 = [x_F + \sqrt{(x_F^2 + 4\tau)}]/2$$
$$x_2 = [-x_F + \sqrt{(x_F^2 + 4\tau)}]/2\,, \tag{4}$$

where

$$x_F = (\vec{p}_{3_L} + \vec{p}_{4_L})/(\sqrt{s}/2)$$
$$\tau = (p_3 + p_4)^2/s\,. \tag{5}$$

In eq. (6), p_3 and p_4 are the 4-momenta of the final two jets and $\vec{p}_{3_L}$ and $\vec{p}_{4_L}$ are the longitudinal momentum components measured along the beam direction in the laboratory frame.

The c.m.s. scattering angle is computed in the rest frame of the final two jets $[(p_3+p_4)]$ relative to the axis defined by the interacting partons $[(\vec{p}_1-\vec{p}_2)]$ assumed massless and collinear with the beams [9]:

$$\cos\theta = (\vec{p}_3 - \vec{p}_4)\cdot(\vec{p}_1 - \vec{p}_2)/(|\vec{p}_3 - \vec{p}_4||\vec{p}_1 - \vec{p}_2|). \quad (6)$$

The finite angular acceptance of the apparatus and the trigger E_T threshold requirement discriminates against events with small scattering angles (i.e. large $\cos\theta$), and restricts the range of $\cos\theta$ over which the trigger is fully efficient. Events which are close to the limits of the acceptance in $\cos\theta$ are rejected by applying a fiducial cut in $\cos\theta$. This fiducial cut ($\cos\theta_{max}$) is defined for each event as the maximum value of $\cos\theta$ for which both the final two jets would fall in the acceptance region $|\eta| < 2.5$ (with at least one jet having $|\eta| < 1.0$) and for which the mean of the transverse energies of the final two jets would exceed (20)35 GeV [in the (un)filtered data set]. Events with azimuthal angle ϕ (defined by the final two jets) within $\pm 45°$ of the vertical, where the two halves of the calorimeter are joined, are also rejected. The final event sample consists of 2432 events satisfying the above cuts, for which the acceptance is essentially uniform.

Figures 1a–d show the raw histograms in $|\cos\theta|$ for various x_1, x_2 intervals. In each case a cut has been applied on $\cos\theta_{max}$ as indicated. The curve, which has been normalized to the number of events in each histogram, shows the expected angular dependence [eq. (2)] assuming vector gluon exchange (QCD). The data are consistent with the curve independent of x_1, x_2 in accordance with eq. (2).

Figure 2 shows the angular distribution obtained using all the events in the sample, on the assumption that the angular dependence is independent of x_1 and x_2. The distribution is computed starting from the raw distributions in $\cos\theta$, classified in intervals of $\cos\theta_{max}$ ($\Delta\cos\theta_{max} = 0.1$), normalizing one distribution to another in the region of overlap. The final distribution is divided by the number of events with $\cos\theta < 0.1$ to obtain $(d\sigma/d\cos\theta)/(d\sigma/d\cos\theta)_{\cos\theta=0}$. Monte Carlo studies demonstrate that, for the range of $\cos\theta$ shown, the angular distribution is not appreciably modified by the effects of resolution smearing. In fig. 2 the data are compared with theoretical forms for gluon–gluon, gluon–quark(antiquark) and quark(antiquark)–quark(antiquark) elastic scattering in QCD (i.e. assuming vector gluon exchange). Theoretical forms for quark(antiquark)–quark(antiquark) and gluon–quark(antiquark) scattering in an Abelian scalar gluon theory [10] are also shown. The data are clearly consistent with the predictions of the vector gluon theory (QCD) and the Abelian scalar gluon theory is excluded. The data are not yet sufficiently accurate, however, to discriminate between the various subprocesses. A fit to the data of the form $(1-\cos\theta)^{-n}$ for $\cos\theta > 0.4$ yields $n = 2.38 \pm 0.10$. This result is close to $n = 2$ and, in analogy with the case of Rutherford scattering at low energy, may be regarded as a test of the inverse square law for the interaction between the partons.

In order to extract the structure function F(x) [eq. (3)] the quantity $S(x_1,x_2)$ is defined in terms of the measured differential cross-section $d^2\sigma/dx_1dx_2$ as follows :

$$S(x_1,x_2) = x_1x_2\,(d^2\sigma/dx_1dx_2)/\textstyle\int_0^{\cos\theta_{max}} K\,(d\sigma/d\cos\theta)\,d\cos\theta\,. \quad (7)$$

If eq. (1) is valid then: $S(x_1,x_2) = F(x_1)\,F(x_2)$. $S(x_1,x_2)$ is determined from the data by weighting the events individually as a function of x_1, x_2, and $\cos\theta_{max}$. The parton–parton differential cross-section $d\sigma/d\cos\theta$ is taken from eq. (2) with $\alpha_s = 12\pi/[23\,\ell n(Q^2/\Lambda^2)]$, i.e. assuming five effective quark flavours and $\Lambda = 0.2$ GeV. For this analysis Q^2 is defined by $Q^2 = -\hat{t}$, where $\hat{t} = (p_1-p_3)^2$ [or $\hat{t} = (p_1-p_4)^2$, whichever is numerically smaller] in analogy with deep inelastic scattering. A factor K has been introduced in eq. (7) to allow for the effect of higher order QCD

corrections, which may change the effective Q^2 scale and hence the normalization of the parton–parton cross-section. These corrections have been computed theoretically [11,12], and are expected to be appreciable even at the energy of the SPS Collider. The results given below have been computed assuming $K = 2$.

The experimental results for $S(x_1,x_2)$ are tabulated in Table 1. The data are symmetric in x_1 and x_2 and have been folded appropriately. The raw event numbers in each bin are given. The data for $\sqrt{\tau} < 0.2$ are based entirely on the unfiltered data set. The data have been corrected for the effects of resolution smearing. This correction varies from -24% at small x to -70% at the largest x values. The quoted errors are statistical only: the systematic error affecting mainly the over-all normalization is $\approx \pm 65\%$, due largely to the uncertainty in the jet energy scale. If factorization holds then $S(x_1,x_2')/S(x_1,x_2)$ will be independent of x_1 for any choice of x_2 and x_2'. This ratio is plotted in Fig. 3a for $x_2 = 0.1$–0.2, $x_2' = 0.05$–0.1 and in Fig. 3b for $x_2 = 0.1$–0.2, $x_2' = 0.2$–0.3. Since the data are symmetric in x_1 and x_2 the folded data (Table 1) have been used to compute the ratio. In each case the ratio is consistent with a constant (broken line) independent of x_1. The data are therefore consistent with factorization in x_1 and x_2.

Figure 4 shows the structure function F(x) [eq. (3)] obtained from $S(x_1,x_2)$ assuming factorization in x_1 and x_2. The results for F(x) are also tabulated in Table 1, together with the mean value of $-\hat{t}$ in each x-bin. The measured integral of F(x) over the range $x = 0.05$–0.80 is 0.53 ± 0.03. The errors quoted are statistical only. Since the cross-section takes the form of a product of structure functions the errors in the structure function are roughly one half the errors in $S(x_1,x_2)$. In particular, the systematic uncertainty in the over-all normalization of the structure function is $\approx \pm 30\%$. Over the range $x = 0.1$–0.8, the data show an exponential x dependence and may be parametrized by the form $F(x) \approx 6.2\, e^{-9.5x}$ (broken line). Over the same range the data cannot be described by a single term of the form $(1-x)^n$ for any choice of n but may be parametrized as the sum of two such terms e.g. $F(x) \approx 8.0\,(1-x)^{13} + 1.1\,(1-x)^4$. Changing the assumed value of Λ by a factor of two (up or down) changes the structure function by $\approx \pm 15\%$. Changing the assumed value of the K-factor [eq. (7)] from $K = 2$ to $K = 1$ increases the structure function by a factor of $\sqrt{2}$, i.e. by an amount comparable to the systematic error.

In fig. 4 the measured F(x) is compared with expectations based on QCD fits to deep inelastic scattering data. The solid curve represents the structure function $G(x) + (4/9)\,[Q(x)+\bar{Q}(x)]$ at $Q^2 = 20$ GeV^2 based on a QCD parametrization of CDHS measurements [13] of G(x) and $[Q(x)+\bar{Q}(x)]$ at low Q^2 ($Q^2 = 2$–200 GeV^2) using a neutrino beam on an iron target. The broken curve shows the expected modification of the structure function, at the value of Q^2 appropriate in this experiment, due to QCD scaling violations (assuming $\Lambda = 0.2$ GeV). The expected contribution due to the quarks and the antiquarks is shown separately. The two-jet data measure directly, for the first time, the very large flux of gluons in the proton at small x ($x \leq 0.3$) and also demonstrate the existence of QCD scaling violations at large Q^2 relative to the low Q^2 data. The present data suggest somewhat softer parton distributions than would be expected based on the CDHS parametrization.

Finally, our result for the integral of F(x) given above may be reinterpreted to yield information on α_s and K. Assuming the validity of the parton model momentum sum-rule we have $\int_0^1 F(x)dx \leq 1$, from which we obtain $\alpha_s\sqrt{K} \geq 0.12$ ($\pm 30\%$ systematic error, due to the uncertainty in the energy scale). It is emphasized that this result is independent of the comparison with deep inelastic scattering data.

Acknowledgements

We gratefully acknowledge the help of the managements and the technical staff of CERN and all outside institutions collaborating in UA1. The following funding agencies in our home countries have contributed to this programme:

Fonds zur Förderung der Wissenschaftlichen Forschung, Austria.
Valtion Luonnontieteellinen Toimikunta, Finland.
Institut National de Physique Nucléaire de Particules,
and Institut de Recherche Fondamentale (CEA), France.
Bundesministerium für Forschung und Technologie, Germany.
Istituto Nazionale di Fisica Nucleare, Italy.
Science and Engineering Research Council, United Kingdom.
Department of Energy, United States of America.

Thanks are also due to the following people who have worked with the collaboration in the preparation and data collection on the runs described here:

F. Bernasconi, F. Cataneo, A.-M. Cnops, L. Dumps, M. Edwards, J.-P. Fournier, A. Micolon, S. Palanque, P. Queru, P. Skimming, G. Stefanini, M. Steuer, J.-C. Thevenin, H. Verweij and R. Wilson.

REFERENCES

1) UA1 Collaboration, G. Arnison et al., Phys. Lett. **123B** (1983) 115.
2) UA2 Collaboration, M. Banner et al., Phys. Lett. **118B** (1982) 203.
   UA2 Collaboration, P. Bagnaia et al., Z. Phys. C **20** (1983) 117.
3) B. Combridge et al., Phys. Lett. **70B** (1977) 234.
4) G. Cohen-Tannoudji et al., preprint SPh.T/70 (1982).
   B. Combridge and C. Maxwell, preprint RL-83-095 (1983).
   F. Halzen and P. Hoyer, Phys. Lett. **130B** (1983) 326.
5) UA1 Collaboration, G. Arnison et al., Phys. Lett. **132B** (1983) 214.
6) M. Della Negra, Physica Scripta **25** (1982) 468.
7) F. Paige and S.D. Protopopescu, ISAJET, BNL 31987.
8) F. Berends et al., Phys. Lett. **103B** (1981) 124.
9) J.C. Collins and D.E. Soper, Phys. Rev. **D16** (1977) 2219.
10) D. Drijard et al., Phys. Lett. **121B** (1983) 433.
11) R.K. Ellis et al., Nucl. Phys. **B173** (1980) 397.
12) N.G. Antoniou et al., Phys. Lett. **128B** (1983) 257.
13) H. Abramowicz et al., Z. Phys. C **12** (1982) 289.
    F. Eisele, private communication.

Table 1

The experimental result for $S(x_1,x_2)$ (see text). The raw event numbers in each x_1,x_2-bin are also given. The quoted errors are statistical only: the systematic error affecting mainly the over-all normalization is $\approx \pm 65\%$.

The corresponding results for F(x) are also tabulated, together with the mean value of $-\hat{t}$ in each x-bin.

$S(x_1,x_2)$

x_1 or x_2	0.05–0.10	0.10–0.20	0.20–0.30	0.30–0.40	0.40–0.50	0.50–0.60	0.60–0.80
0.05–0.10	-	-	3.053 ± 0.276 (340)	1.224 ± 0.207 (225)	0.449 ± 0.122 (145)	0.298 ± 0.134 (66)	0.064 ± 0.038 (38)
0.10–0.20	-	2.541 ± 0.247 (263)	0.842 ± 0.118 (392)	0.373 ± 0.061 (202)	0.218 ± 0.047 (115)	0.055 ± 0.027 (30)	0.024 ± 0.015 (16)
0.20–0.30	-	-	0.391 ± 0.080 (75)	0.117 ± 0.044 (28)	0.038 ± 0.029 (13)	0.032 ± 0.038 (11)	0.005 ± 0.011 (1)
0.30–0.40	-	-	-	0.042 ± 0.053 (3)	0.022 ± 0.040 (3)	0.009 ± 0.028 (1)	0.000 ± 0.000 (0)

F(x)

F(x)	5.497 ± 0.578	1.607 ± 0.082	0.542 ± 0.049	0.222 ± 0.030	0.112 ± 0.027	0.038 ± 0.017	0.012 ± 0.006
$\langle -\hat{t} \rangle$ GeV^2	1500	2200	3000	4100	4100	4600	5100

Figure captions

Fig. 1 : a–d) Histograms in cos θ for various x_1, x_2 intervals. A cut on cos θ_{max} has been applied as indicated. The curve, which has been normalized to the number of events in each histogram, is the expected angular dependence [eq. (2)] assuming vector gluon exchange (QCD).

Fig. 2 : The angular distribution obtained using all the events in the sample on the assumption that the angular dependence is independent of x_1 and x_2. The data are compared with theoretical forms for parton–parton elastic scattering in QCD and in an Abelian scalar gluon theory [9].

Fig. 3 : The ratio $S(x_1,x_2')/S(x_1,x_2)$ for a) $x_2 = 0.1$–0.2, $x_2' = 0.05$–0.1 and b) $x_2 = 0.1$–0.2, $x_2' = 0.2$–0.3. In each case the data are consistent with a constant (broken line) independent of x_1.

Fig. 4 : The structure function of F(x) [eq. (3)]. The errors are statistical only: the systematic error affecting mainly the over-all normalization is $\approx \pm 30\%$. The broken line represents the parametrization $F(x) = 6.2\, e^{-9.5x}$ (see text). The solid curve represents a QCD parametrization of the structure function $G(x) + (4/9)\,[Q(x)+\bar{Q}(x)]$ at $Q^2 = 20\ GeV^2$ based on the CDHS [13] measurements at low Q^2 ($Q^2 = 2$–$200\ GeV^2$). The broken curves show the expected modification of the structure function at the values of Q^2 appropriate in this experiment. The expected contribution of quarks and antiquarks is shown separately.

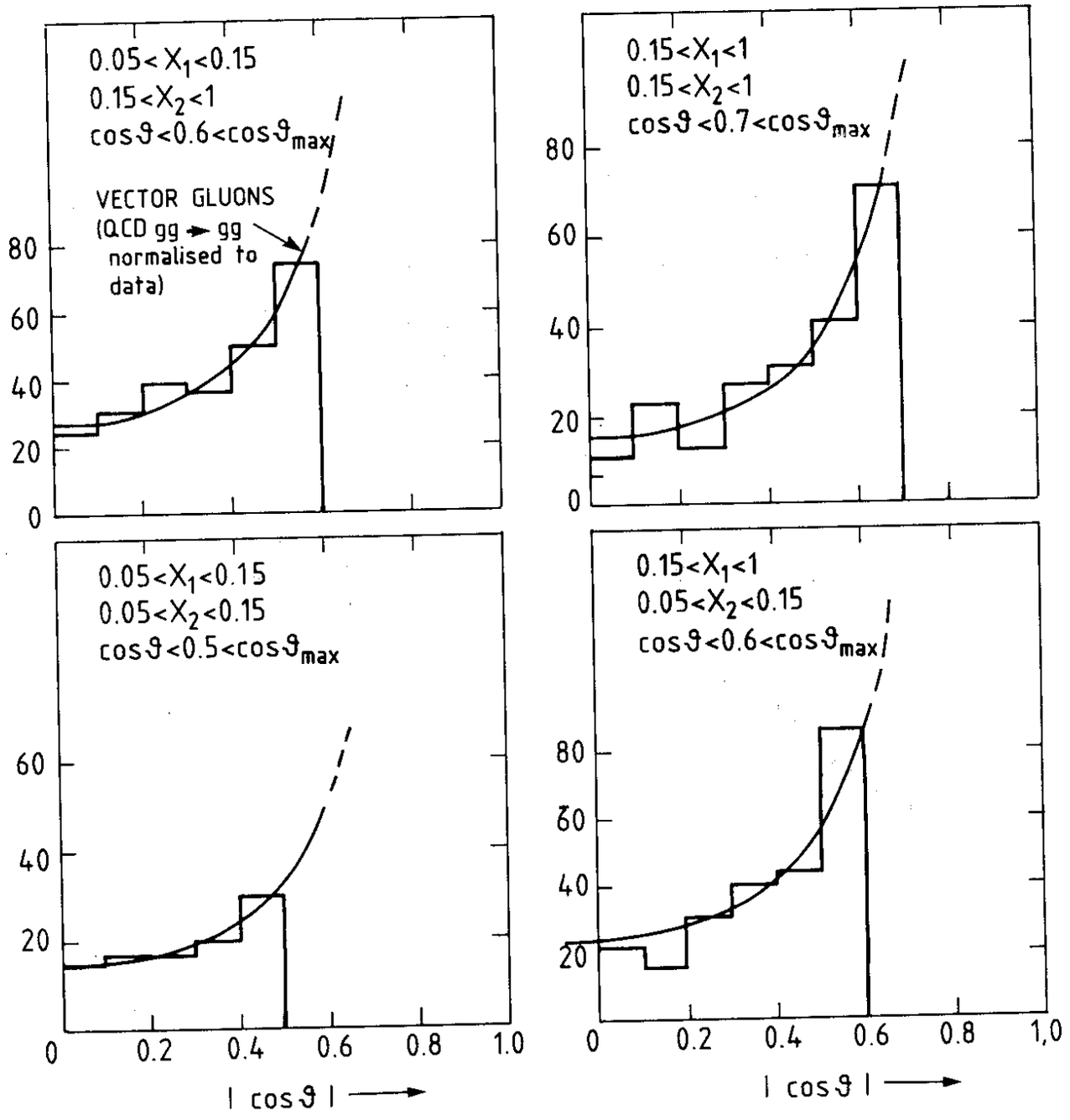
0.05< X1<0.15
0.15<X2<1
cos ϑ <0.6<cos ϑmax
VECTOR GLUONS
(QCD gg → gg
normalised to
data)
0.15<X1<1
0.15<X2<1
cos ϑ <0.7<cos ϑmax
0.05<X1<0.15
0.05<X2<0.15
cos ϑ <0.5<cos ϑmax
0.15<X1<1
0.05<X2<0.15
cos ϑ <0.6<cos ϑmax
0
20
40
60
80
0.2
0.4
0.6
0.8
1.0
| cos ϑ |

Fig. 1

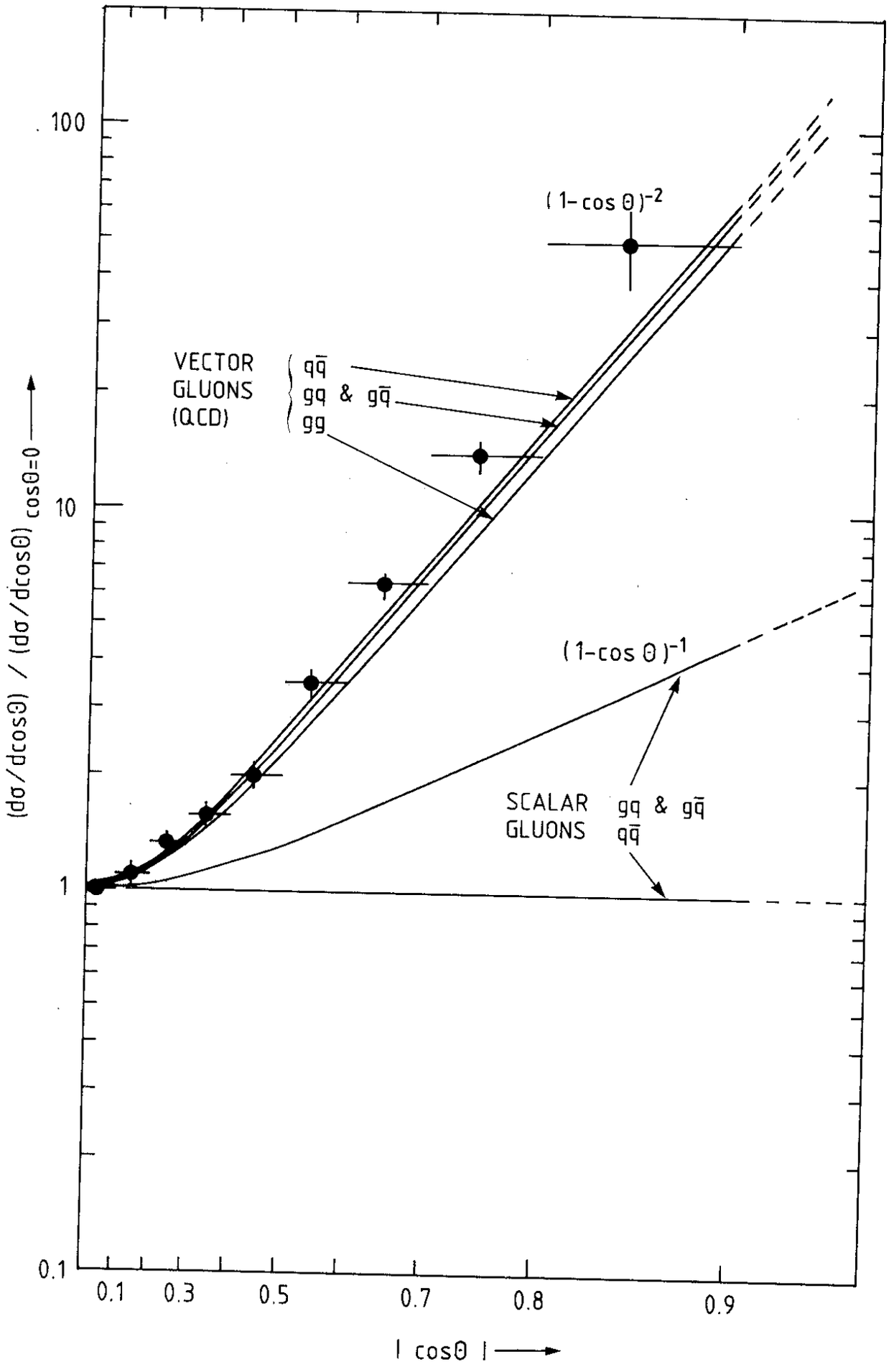
100
10
1
0.1
0.1
0.3
0.5
0.7
0.8
0.9
(dσ/dcosΘ) / (dσ/dcosΘ) cosΘ=0
| cosΘ |
(1-cos Θ)-2
VECTOR GLUONS (QCD)
qq̄
gq & gq̄
gg
(1-cos Θ)-1
SCALAR GLUONS
gq & gq̄
qq̄

Fig. 2

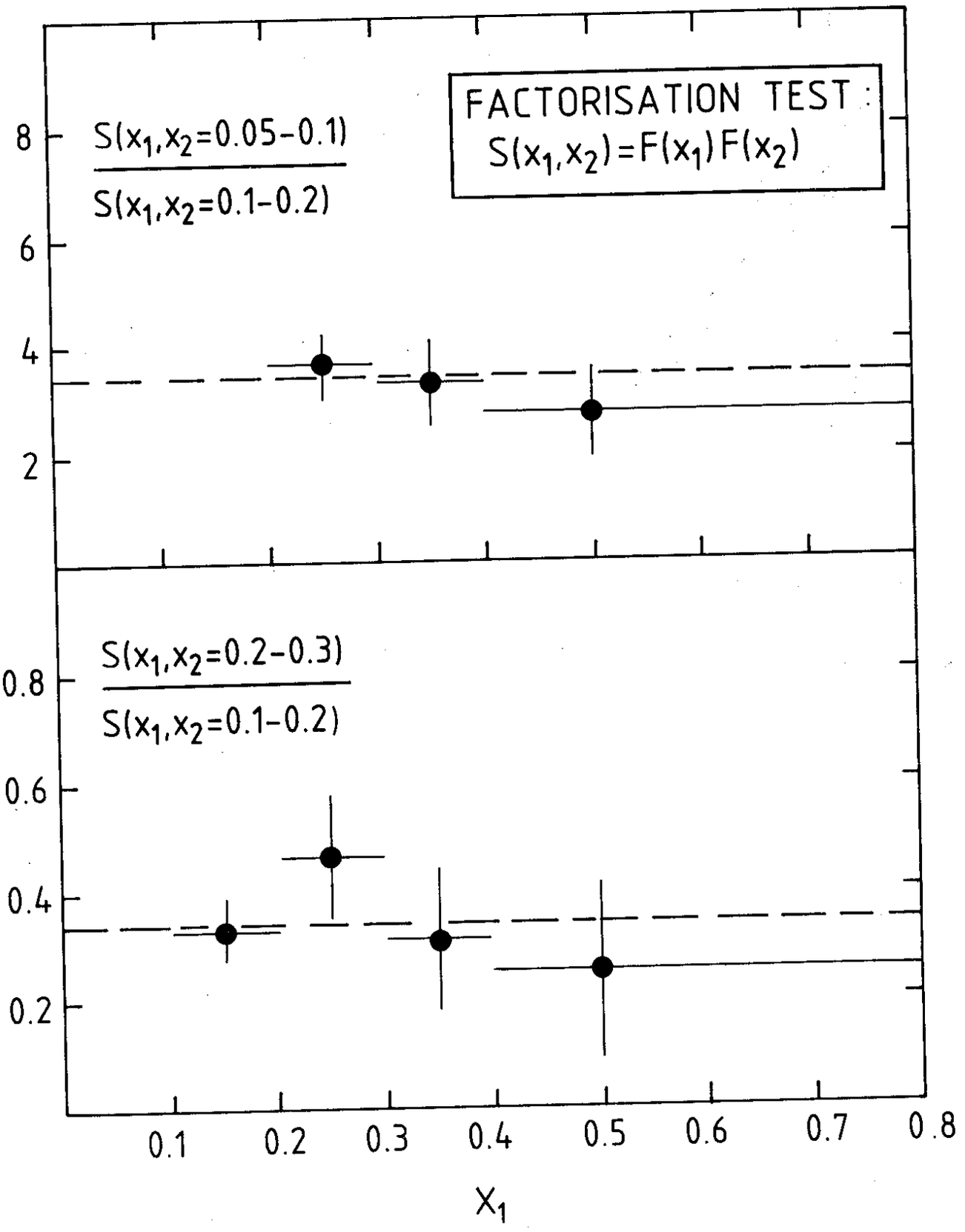
FACTORISATION TEST :
$S(x_1,x_2) = F(x_1)F(x_2)$
$\frac{S(x_1,x_2=0.05-0.1)}{S(x_1,x_2=0.1-0.2)}$
$\frac{S(x_1,x_2=0.2-0.3)}{S(x_1,x_2=0.1-0.2)}$
8
6
4
2
0.8
0.6
0.4
0.2
0.1
0.2
0.3
0.4
0.5
0.6
0.7
0.8
X_1

Fig. 3

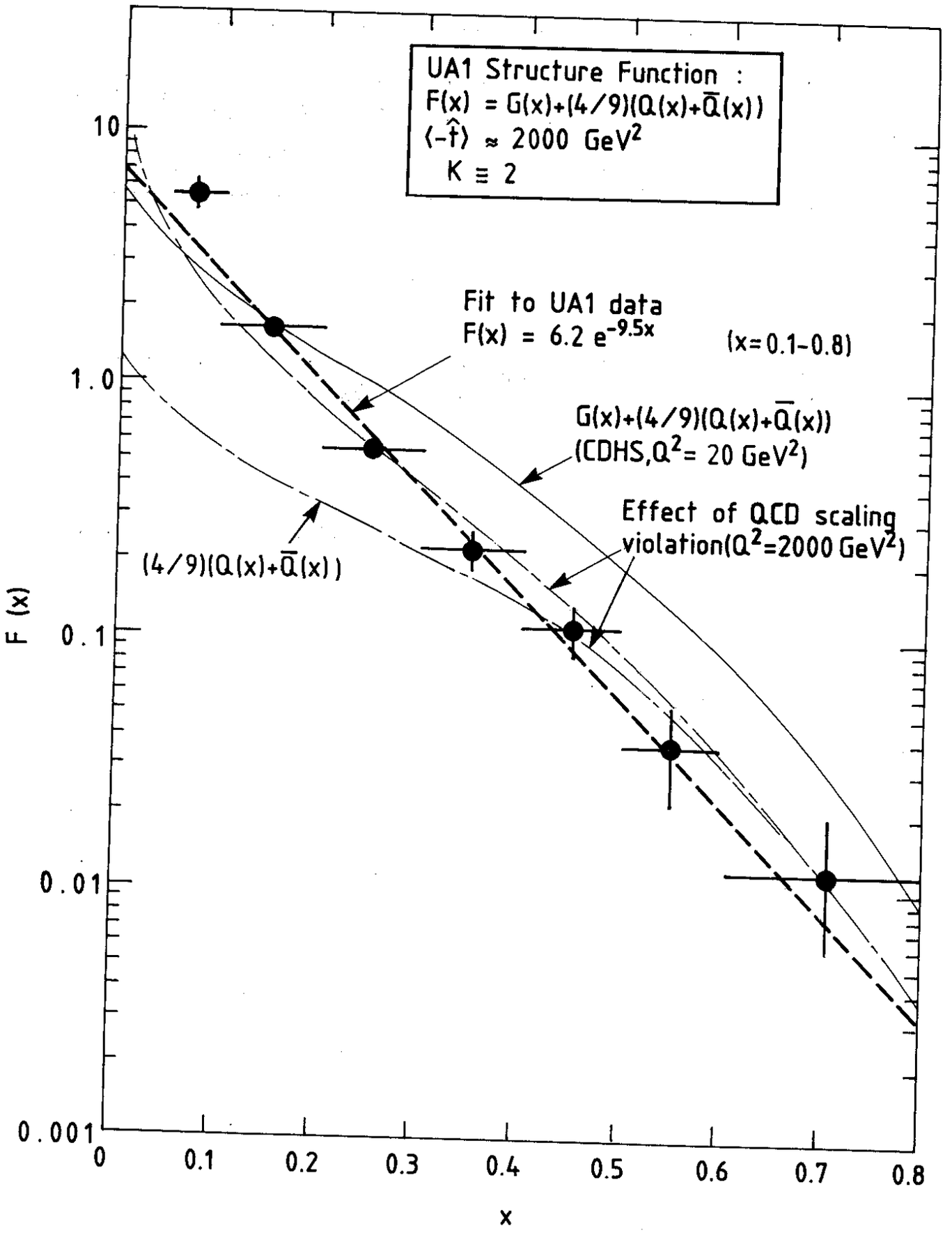
UA1 Structure Function :
F(x) = G(x)+(4/9)(Q(x)+Q̄(x))
⟨-t̂⟩ ≈ 2000 GeV²
K ≡ 2
Fit to UA1 data
F(x) = 6.2 e^-9.5x
(x=0.1-0.8)
G(x)+(4/9)(Q(x)+Q̄(x))
(CDHS,Q²= 20 GeV²)
Effect of QCD scaling
violation(Q²=2000 GeV²)
(4/9)(Q(x)+Q̄(x))
F (x)
10
1.0
0.1
0.01
0.001
0
0.1
0.2
0.3
0.4
0.5
0.6
0.7
0.8
x

Fig. 4